

Many-body stabilization of a resonant p-wave Fermi gas in one dimension

Lei Pan,^{1,2} Shu Chen,^{1,2,3} and Xiaoling Cui^{1,*}

¹*Beijing National Laboratory for Condensed Matter Physics,
Institute of Physics, Chinese Academy of Sciences, Beijing 100190, China*

²*University of Chinese Academy of Sciences, Beijing 100049, China*

³*Collaborative Innovation Center of Quantum Matter, Beijing, China*

(Dated: December 3, 2024)

Using the asymptotic Bethe ansatz method, we study the stabilization problem of the one-dimensional spin-polarized Fermi gas confined in a hard-wall potential with tunable p-wave scattering length and finite effective range. We find that the interplay of two factors, i.e., the finite interaction range and the hard-wall potential, will help to stabilize the system near resonance. The stabilization occurs even in the positive scattering length side, where the system undergoes a many-body collapse if any of the factors is absent. In particular, at p-wave resonance, the system is stabilized if the finite range is above twice the mean particle distance. Slightly away from resonance, we extract the lowest-order correction to the stability condition in terms of the inverse scattering length. Finally, we present a global picture for the energetics and the stability property of fermions from weakly attractive to deep bound state regime. Our results suggest a many-body stable p-wave Fermi gas is within the reach of current cold atoms techniques.

Introduction. Experimental realization of p-wave ultracold Fermi gases with tunable interactions[1–6] offers great opportunities for investigating many intriguing p-wave phenomena, such as the rich orbital pairing and the topological superfluids[7–11]. At this stage, a central issue for the experimental detection of low-energy p-wave physics is the severe atom loss near resonance, which prohibits the many-body equilibration in a reasonably long time scale. In 3D and quasi-2D, the loss mainly comes from the strong inelastic three-body collision, which is associated with the presence of centrifugal barrier for two-body collision and the resulted shallow molecules that are highly weighted at short-range and easily decay to deep molecules. While such loss is likely to be suppressed in quasi-1D given the spatially extended molecule near resonance[12], there can be another source for the loss in 1D, i.e., the many-body collapse due to negative compressibility. This is inferred from the theorem of Bose-Fermi duality [13], which maps the wave functions and the energies between p-wave fermions and s-wave bosons with inverse coupling strengths [13–15]. Accordingly, the p-wave fermions with a positive scattering length (where a two-body molecule is supported) can be mapped to attractive bosons, thereby implying the fermions immediately undergo a many-body collapse once across resonance to the molecule side.

Nevertheless, in drawing above conclusion we have missed an important ingredient, which is the finite effective range. The Bose-Fermi duality only applies to zero range case but not finite range[16]. In practice, the p-wave Feshbach resonance generally has a large effective range in 3D[2, 6], which results in a large range in quasi-1D through the confinement-induced resonance[17–20]. Previous studies have shown that the effective range can significantly change the property of 1D p-wave Fermi gas with periodic boundary in the negative scattering length

side[21, 22], where the system is known to be stable. The system has also been exactly treated in the same interaction regime in a hard-wall potential without range[23]. As it is generally believed that the fermions with a positive scattering length are unstable, there have been rare discussions of the many-body physics in this regime[24].

In this work, we focus on the energetics and the stability property of 1D fermions across p-wave resonance, in both positive and negative sides, with a finite interaction range and in a hard-wall potential. We have exactly solved the system using the asymptotic Bethe ansatz method. It is found that the interplay of the finite range and the hard-wall potential helps to stabilize the system even in the positive scattering length side, where the system would undergo a many-body collapse if any of the two factors is absent. In particular, at p-wave resonance, the system is stabilized if the range is above twice the mean particle distance. Slightly away from resonance, the correction to the stability condition linearly depends on the inverse scattering length, which can be extracted from the analysis of Bethe ansatz equations. Furthermore, we present a global picture for the energetics and the stability property of the system from weakly attractive to deep bound state regime. Our results can be directly detected in the quasi-1D cold Fermi gas with an additional box-trap potential.

Formalism. To determine the low-energy physics in the quasi-1D regime, i.e., when $E \ll \omega_{\perp}$ (ω_{\perp} is the frequency of transverse harmonic confinement), we utilize the following boundary condition for the many-body wave function when a pair of fermions come close to each other[21, 22]:

$$\lim_{x \equiv x_j - x_i \rightarrow 0^+} \left(\frac{1}{l_p} + \partial_x - \xi_p \partial_x^2 \right) \Psi(x_1, x_2, \dots, x_N) = 0. \quad (1)$$

Here l_p and ξ_p are, respectively, the reduced 1D p-wave

scattering length and effective range[17–20], and $\{x_i\}$ ($i = 1, \dots, N$) are the coordinates of N spin-polarized fermions. The many-body wave function Ψ takes the form:

$$\Psi = \sum_Q \theta(x_{q_N} > x_{q_{N-1}} \dots > x_{q_1}) \varphi_Q(x_{q_1}, x_{q_2}, \dots, x_{q_N}) \quad (2)$$

where Q labels the region $0 \leq x_{q_1} \leq x_{q_2} \leq \dots \leq x_{q_N} \leq L$ and φ_Q is the wave function in this region. To ensure the antisymmetry of Ψ , we have $\varphi_Q(\dots x_i, \dots x_j, \dots) = -\varphi_Q(\dots x_j, \dots x_i, \dots)$. Here we consider the system confined in a hard-wall potential (with length L), which satisfies the open boundary condition(OBC)

$$\varphi_Q(0, x_{q_2}, \dots, x_{q_N}) = \varphi_Q(x_{q_1}, x_{q_2}, \dots, L) = 0 \quad (3)$$

$$\varphi_Q = (-1)^Q \sum_P (-1)^P A_P \exp \left[i \left(\sum_{l < j}^{N-1} \omega_{p_j p_l} \right) + i k_{p_N} L \right] \sin(k_{p_1} x_{q_1}) \prod_{1 < j < N} \sin \left(k_{p_j} x_{q_j} - \sum_{l < j} \omega_{p_l p_j} \right) \sin(k_{p_N} (x_{q_N} - L)) \quad (4)$$

with $\omega_{ab} = \arctan \frac{\frac{\xi_p}{2}(k_a - k_b)^2 + \frac{2}{l_p}}{k_a - k_b} - \arctan \frac{\frac{\xi_p}{2}(k_a + k_b)^2 + \frac{2}{l_p}}{k_a + k_b}$, and $A_{p_1 p_2 \dots p_N} = \prod_{j < l}^N \left(i k_{p_j} - i k_{p_l} + [\frac{\xi_p}{2}(k_{p_j} - k_{p_l})^2 + \frac{2}{l_p}] \right) \left(i k_{p_j} + i k_{p_l} + [\frac{\xi_p}{2}(k_{p_j} + k_{p_l})^2 + \frac{2}{l_p}] \right)$. Here $(-1)^Q = \pm 1$ and $(-1)^P = \pm 1$ denote sign factors associated with even/odd permutations of $Q = (q_1, q_2, \dots, q_N)$ and $P = (p_1, p_2, \dots, p_N)$, respectively. Apparently φ_Q satisfies the OBC (3).

For zero-range case ($\xi_p = 0$), one can see that Eq.5 directly reduces to the BAE of identical bosons with coupling $c = -2/l_p$ [24], hence the two systems have the same quasi- k distribution and thus the same E , as is exactly predicted by the Bose-Fermi duality[13]. However, when turn on a finite range ($\xi_p \neq 0$), Eq.5 can no longer be reduced to the BAE of the finite-range bosons, due to the distinct forms of energy-dependent coupling strengths for the two systems[12], and thus the duality breaks down. As a result, the physics we will address below for the finite-range fermions will have no correspondence in finite-range bosons[26, 27]. In the rest of the paper, we will use L and $E_0 = (2mL^2)^{-1}$ as the unit of length and energy respectively.

At resonance. We first analyze the range effect at resonance ($1/l_p = 0$). In this case, the BAEs (5) support a ground state with all equal $k_j \equiv k$, which lead to a single

According to the Bethe ansatz method, we expand

$$\varphi_Q(x_{q_1}, x_{q_2}, \dots, x_{q_N}) = \sum_{P, \{r_j\}} \left[A_P \exp \left(i \sum_j r_j k_{P_j} x_{q_j} \right) \right] \quad (4)$$

Here $r_j = \pm 1$ denotes the j -th particle moving to right and left. Substituting Eq.(4) into Eq.(2) and applying the boundary conditions Eqs.(1,3), we can obtain the following Bethe ansatz equations(BAEs):

$$e^{i 2 k_j L} = \prod_{l \neq j} \frac{i(k_j - k_l) + \left[\frac{\xi_p}{2}(k_j - k_l)^2 + \frac{2}{l_p} \right]}{i(k_j - k_l) - \left[\frac{\xi_p}{2}(k_j - k_l)^2 + \frac{2}{l_p} \right]} \times \frac{i(k_j + k_l) + \left[\frac{\xi_p}{2}(k_j + k_l)^2 + \frac{2}{l_p} \right]}{i(k_j + k_l) - \left[\frac{\xi_p}{2}(k_j + k_l)^2 + \frac{2}{l_p} \right]} \quad (5)$$

Here k_j ($j = 1, \dots, N$) is the quasi-momentum, which gives the eigen-energy $E = \sum_{j=1}^N k_j^2 / (2m)$. Compared to the BAEs under periodic boundary condition (PBC)[21, 22, 25], here Eq.5 include an additional term representing the reflection of particles at the hard-wall boundary.

Accordingly, the wavefunction $\varphi_Q(x_{q_1}, x_{q_2}, \dots, x_{q_N})$ is

closed equation for k :

$$k = \pi - (N - 1) \arctan(\xi_p k). \quad (7)$$

Accordingly, the wave function simply reduces to

$$\varphi_Q(x_{q_1}, x_{q_2}, \dots, x_{q_N}) \sim \prod_{j=1}^N \sin \left[k x_{q_j} - (j - 1) \frac{k - \pi}{N - 1} \right]. \quad (8)$$

In the case of $\xi_p = 0$, we have $k = \pi$ and $\varphi_Q \sim \prod_j \sin(\pi x_{q_j})$, which means all quasi-particles condense at the lowest single-particle state with zero-point energy $E = N\pi^2$. This can be easily understood in the framework of Bose-Fermi duality, namely, the bosons condense at the lowest energy state in the non-interacting limit. Remarkably, when tune on a finite range $\xi_p > 0$, the picture of quasi-particle condensation still applies since all quasi- k are still identical, while in the wave function (8) each quasi-particle has a different phase shift from left to

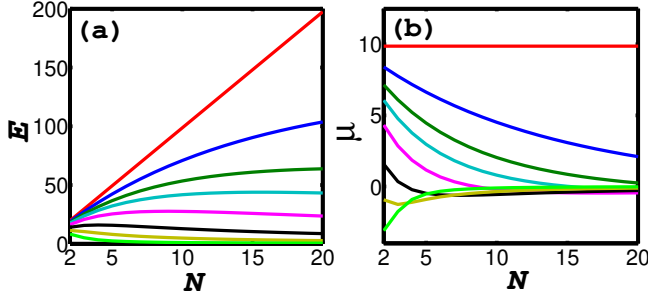


FIG. 1. (color online) Ground state energy E (a) and chemical potential μ (b) as functions of N at p-wave resonance. Several different ranges are chosen as (from top to bottom): $\xi_p = 0, 0.02, 0.04, 0.06, 0.1, 0.2, 0.4, 1.0$. The units of length and energy are L and $E_0 = (2mL^2)^{-1}$, respectively.

right in the coordinate space, such that the OBC (3) can be satisfied.

For large N , Eq.(7) gives the solution $k = \pi/[1 + (N - 1)\xi_p]$, and the total energy is

$$E = \frac{N\pi^2}{[1 + (N - 1)\xi_p]^2}. \quad (9)$$

Therefore E will decrease all along as increasing ξ_p . This can be understood in terms of the energy-dependent scattering length $l_p^{-1}(k) = l_p^{-1} + \xi_p k^2$: because of the zero-point energy in a hard-wall potential, the lowest collision energy ($\sim k^2$) are generally positive, which gives a stronger effective interaction, i.e., larger $l_p^{-1}(k)$ as increasing ξ_p , and results in a lower energy E . This is to be contrast with the PBC case where the zero-point energy is absent, and we have checked that in this case the fermion energy always stays at zero regardless of ξ_p .

Importantly, the energy expression (9) also suggests a tunable stability by ξ_p . From (9), one can easily derive the chemical potential $\mu = \partial E / \partial N$ and the inverse compressibility $\chi^{-1} = \partial^2 E / \partial N^2$ as:

$$\mu = \frac{\pi^2 [1 - (N + 1)\xi_p]}{[1 + (N - 1)\xi_p]^3}; \quad (10)$$

$$\chi^{-1} = \frac{2\pi^2 \xi_p [(N + 2)\xi_p - 2]}{[1 + (N - 1)\xi_p]^4}. \quad (11)$$

Therefore the system will become stable with $\chi > 0$ under the condition

$$\xi_p > \xi_{p,c} = \frac{2}{N + 2}. \quad (12)$$

In extremely large N limit, $\xi_{p,c} \rightarrow 2d$ where $d = 1/N$ is the mean inter-particle distance (here the length unit is the system size L).

In Fig.1(a,b), we plot $E(N)$ and $\mu(N) = E(N + 1) - E(N)$ of the ground state by solving Eq.(7) for different

values of ξ_p . We can see that as ξ_p increases from zero, E gradually decreases from the zero-point energy $N\pi^2$, and even changes the curvature as a function of N . Accordingly, μ changes from a constant π^2 to a varying function of N . When ξ_p is above a critical value $\xi_{p,c}$, the slope of $\mu \sim N$ changes from negative to positive, implying that the system becomes stable with a positive compressibility. In Fig.2(a), we show the numerical value of $\xi_{p,c}$ as a function of N , which fits well with the analytical prediction (12).

Near resonance. We now turn to the near resonance regime, i.e., $1/l_p \rightarrow 0^\pm$, and we will extract the correction to E and to the stability condition up to the lowest order of $1/l_p$. Away from resonance, the quasi-momenta k_j are no longer identical but depend on j . In the regime $1/l_p \rightarrow 0^-$, all k_j are real and can be expanded as $k_j = k + c_j|l_p|^{-1/2} + d_j|l_p|^{-1}$; here k is the solution at $1/l_p = 0$ following Eq.(7). By expanding the BAEs (5) up to the order of $1/l_p$, we obtain the following equations for $\{c_j\}$ and $\{d_j\}$:

$$c_j = \sum_{l \neq j} \left(\frac{2}{c_j - c_l} - \frac{\xi_p}{2} (c_j - c_l) - \frac{\xi_p}{2} \frac{c_j + c_l}{1 + (k\xi_p)^2} \right); \quad (13)$$

$$d_j = \sum_{l \neq j} \left(F_{jl} + G_{jl} + \frac{1}{1 + (k\xi_p)^2} \left[\frac{1}{k} - \frac{\xi_p}{2} (d_j + d_l) \right] \right) \quad (14)$$

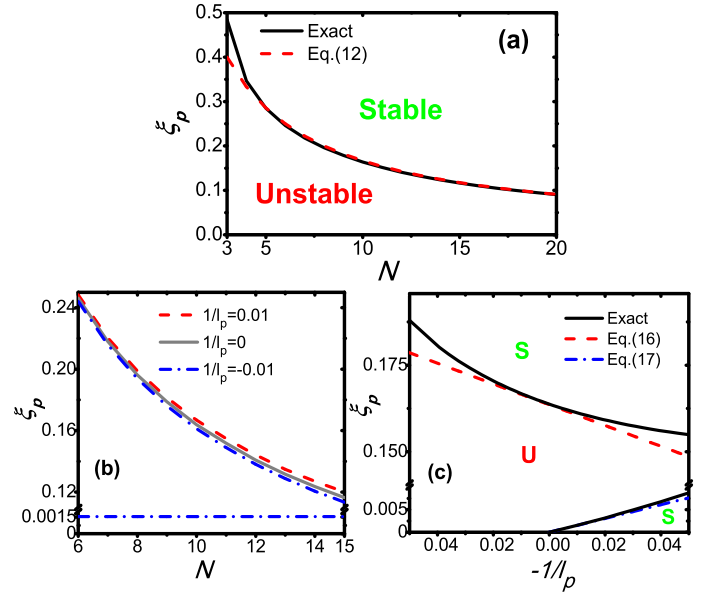


FIG. 2. (color online) (a) Critical effective range $\xi_{p,c}$ as functions of N at resonance. The system is stable (unstable) when ξ_p is above (below) $\xi_{p,c}$. Red dashed line shows the analytical fit according to Eq.(12). (b) $\xi_{p,c}$ as functions of N near resonance at $1/l_p = 0.01$ (red dashed) and at $1/l_p = -0.01$ (blue dash-dot). For comparison, $\xi_{p,c}$ at resonance are shown as gray line. (c) $\xi_{p,c}$ as changing $1/l_p$ for $N = 10$. "S" and "U" denote respectively the stable and unstable regions. The red dashed and blue dash-dot lines show linear fits to Eq.(16) and Eq.(17) respectively.

with $F_{jl} = -(d_j - d_l)(\xi_p/2 + 2(c_j - c_l)^{-2})$, $G_{jl} = (c_j + c_l)^2 k \xi_p^3 / [4(1 + k \xi_p^2)^2]$. In the regime $1/l_p \rightarrow 0^+$, k_j has imaginary part scaling as $l_p^{-1/2}$ and by expanding it as $k_j = k + i c_j l_p^{-1/2} - d_j l_p^{-1}$, we have $\{c_j\}$ and $\{d_j\}$ satisfy the same sets of equations as (13,14). Therefore the energy correction up to the order of $1/l_p$ has a unified form for different sides of resonance, i.e., $\Delta E = (-1/l_p) \sum_j (c_j^2 + 2k d_j)$.

In the case of $\xi_p = 0$, we have $c_j = \sum_{l \neq j} \frac{2}{c_j - c_l}$ and $d_j = (N-1)/\pi$, thus the energy correction $\Delta E = (-1/l_p) 3N(N-1)$ is identical to the interaction energy of weakly interacting bosons, consistent with the Bose-Fermi duality. When $\xi_p \neq 0$, the situation can be simplified in large N limit, where $k \xi_p \ll 1$ and F_{jl} , G_{jl} are negligible compared to the last term in Eq.(14). In this case, we have $[1 + (N-1)\xi_p]c_j = \sum_{l \neq j} \frac{2}{c_j - c_l}$ and $d_j = (N-1)/(k[1 + (N-1)\xi_p])$, and the energy correction is

$$\Delta E = -\frac{1}{l_p} \frac{3N(N-1)}{[1 + (N-1)\xi_p]}. \quad (15)$$

Given ΔE , we obtain the stability condition near resonance:

$$\xi_p > \xi_{p,c}^{\text{res}} + \frac{9N^2}{2\pi^2(N+2)^2} \frac{1}{l_p}; \quad (16)$$

here $\xi_{p,c}^{\text{res}}$ is the critical value at resonance. In addition, for $1/l_p \rightarrow 0^-$ the system has an extra stable region:

$$\xi_p < -\frac{3}{2\pi^2} \frac{1}{l_p}. \quad (17)$$

These results suggest that even in the positive side of resonance, the system can still be stable against collapse in a sizable region of ξ_p . In Fig.2(b), we plot the critical $\xi_{p,c}$ as function of N for two small $1/l_p$ at both sides of resonance, and we find $\xi_{p,c}$ are indeed only slightly deviated from the resonance value $\xi_{p,c}^{\text{res}}$ (the gray line). In Fig.2(c), we show $\xi_{p,c}$ for a given $N = 10$ as changing $1/l_p$ near resonance, and the numerical results fit well with analytical predictions in Eqs.(16,17). We remark that such stability property is very different from the PBC case or the zero-range case, where the system immediately becomes unstable (with $\chi < 0$) once across resonance to the positive side. Therefore the stabilization is facilitated by the interplay of both factors, namely, the finite range and the external (hard-wall) confinement.

Far from resonance. Further departing from resonance, above results will become invalid when the next-order correction to the energy ($\sim N^3/l_p^2$) dominates over the lowest one ($\sim N^2/l_p$) roughly at $|l_p| < N$. In the weak coupling limit $l_p \rightarrow 0^-$, the BAEs (5) give the linear expansion of k_j around the non-interacting value: $k_j = j\pi(1 + (N-1)l_p)$, and this leads to

$$E = E^{(0)} \left[1 + 2(N-1)l_p + o(l_p^2) \right], \quad (18)$$

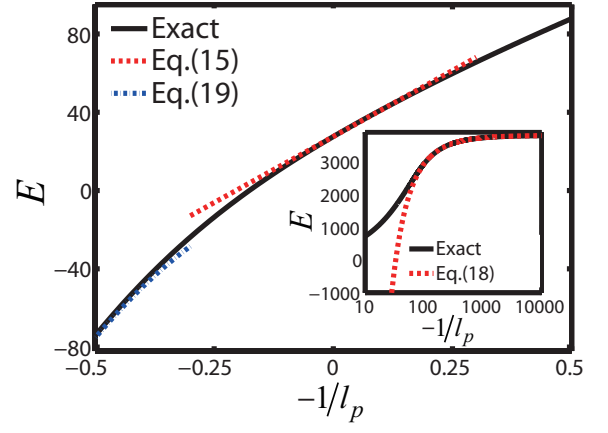


FIG. 3. (Color online) Ground state energy E as a function of interaction strength $-1/l_p$ for $\xi_p = 0.1$ at $N = 10$. The red dashed line shows the linear fit near resonance based on Eq.(15), and the blue dash-dot line shows the generalized string solution (19). Inset: E in the extremely weak coupling regime, fitted by the perturbation result (18) (see red dashed).

where $E^{(0)} = \pi^2 N(N+1)(2N+1)/6$ is the non-interacting Fermi sea energy. Indeed, the energy expansion (18) can also be obtained through the first-order perturbation theory based on the pseudo-potential $U = \sum_{i,j} (2l_p/m) \partial_{x_{ij}} \delta(x_{ij}) \partial_{x_{ij}}$ and an unperturbed Fermi sea. In this limit, the effective range plays negligible role and the system is always stable.

In the deep bound state limit $l_p \rightarrow 0^+$, we generalize the N -string solution of attractive bosons[23, 24] to the present system as $k_j = \alpha + i(N+1-2j)\sqrt{E_{2b}}$, where $E_{2b} = (1 + 2\xi_p/l_p - \sqrt{1 + 4\xi_p/l_p})/(2\xi_p^2)$ is the two-body binding energy. For large N , the total energy is mainly contributed from the imaginary part of the string solution and is given by

$$E = -\frac{N(N^2-1)}{3} E_{2b}, \quad (19)$$

which represents a cluster bound state. In this limit, the system is always unstable for any values of ξ_p .

In Fig.3, we plot E as function of $-1/l_p$ for a finite range $\xi_p = 0.1$ at $N = 10$. We can see that E increases all along with $-1/l_p$, and the exact solutions can be well fitted by analytical results in the weak-coupling limit (18), near resonance (15), and the cluster bound state limit (19). Given all above analyses, we conclude that a finite range will play the most essential role in the resonance regime, where both the energetics (9,15) and the stability property (12,16,17) of the system can be significantly modified by the range effect.

Summary and discussion. In summary, we have shown that a 1D spin-polarized Fermi gas can be stabilized near p-wave resonance (in both sides) in the presence of a finite range and a hard-wall potential, in contrast to the zero-range or periodic boundary condition case where a many-body collapse occurs once across resonance to the positive

side. The modified energetics and stability property as revealed in this work suggest a new avenue of research for 1D systems, in particular, when the Bose-Fermi duality breaks down.

Our results can be directly tested in the quasi-1D ^{40}K or ^6Li Fermi gas with an additional box-trap potential[28] along the (1D) free direction. Take the ^{40}K Fermi gas near 200G for example, according to the most updated expression for ξ_p [12], we have $\xi_p = 250 \sim 950\text{nm}$ for the transverse confinement length $a_\perp = 60 \sim 120\text{nm}$. Therefore ξ_p can be tuned to stay below or above twice the mean inter-particle distance d , which is typically hundreds of nanometers, and thus the stability can be conveniently tuned by ξ_p or d (according to Eqs.(12,16)).

Acknowledgment. The work is supported by the National Natural Science Foundation of China (No.11622436, No.11425419, No.11421092, No.11534014), the National Key Research and Development Program of China (2016YFA0300603).

* xlcul@iphy.ac.cn

- [1] C. A. Regal, C. Ticknor, J. L. Bohn, and D. S. Jin, Phys. Rev. Lett. **90**, 053201 (2003).
- [2] C. Ticknor, C. A. Regal, D. S. Jin, and J. L. Bohn, Phys. Rev. A **69**, 042712 (2004).
- [3] J. Zhang, E. G. M. van Kempen, T. Bourdel, L. Khaykovich, J. Cubizolles, F. Chevy, M. Teichmann, L. Tarruell, S. J. J. M. F. Kokkelmans, and C. Salomon, Phys. Rev. A **70**, 030702 (R)(2004).
- [4] C. H. Schunck, M. W. Zwierlein, C. A. Stan, S. M. F. Raupach, W. Ketterle, A. Simoni, E. Tiesinga, C. J. Williams, and P. S. Julienne, Phys. Rev. A **71**, 045601 (2005).
- [5] K. Gunter, T. Stoferle, H. Moritz, M. Kohl, and T. Esslinger, Phys. Rev. Lett. **95**, 230401 (2005).
- [6] C. Luciuk, S. Trotzky, S. Smale, Z. Yu, S. Zhang, J. H. Thywissen, Nature Physics **12**, 599 (2016).
- [7] V. Gurarie, L. Radzihovsky, and A.V. Andreev, Phys. Rev. Lett. **94**, 230403 (2005).
- [8] C.-H. Cheng and S.-K. Yip, Phys. Rev. Lett. **95**, 070404 (2005).
- [9] N. Read and D. Green, Phys. Rev. B **61**, 10267 (2000).
- [10] S. Tewari, S. Das Sarma, C. Nayak, C. Zhang and P. Zoller, Phys. Rev. Lett. **98**, 010506 (2007).
- [11] A.Y. Kitaev, Phys. Usp. **44**, 131 (2001).
- [12] L. Zhou and X. Cui, Phys. Rev. A **96**, 030701 (R) (2017).
- [13] T. Cheon and T. Shigehara, Phys. Rev. Lett. **82**, 2536 (1999); Phys. Lett. A **243**, 111 (1998).
- [14] M. D. Girardeau, H. Nguyen, and M. Olshanii, Opt. Commun. **243**, 3 (2004).
- [15] S. A. Bender, K. D. Erker, and B. E. Granger, Phys. Rev. Lett. **95**, 230404 (2005).
- [16] X. Cui, Phys. Rev. A **94**, 043636 (2016).
- [17] B. E. Granger and D. Blume, Phys. Rev. Lett. **92**, 133202 (2004).
- [18] L. Pricoupenko, Phys. Rev. Lett. **100**, 170404 (2008).
- [19] S.-G. Peng, S. Tan, and K. Jiang, Phys. Rev. Lett. **112**, 250401 (2014).
- [20] Full expressions of the reduced 1D p-wave scattering length and effective range are given in Ref.[12].
- [21] A. Imambekov, A. A. Lukyanov, L. I. Glazman, and V. Gritsev, Phys. Rev. Lett. **104**, 040402 (2010).
- [22] X.-L. Chen, X.-J. Liu, H. Hu, Phys. Rev. A **94**, 033630 (2016).
- [23] Y. Hao, Y. Zhang, and S. Chen, Phys. Rev. A **76**, 063601 (2007).
- [24] M. Takahashi, Thermodynamics of One-Dimensional Solvable Models (Cambridge University Press, Cambridge, England, 1999).
- [25] Note that the first terms in the right side of our BAEs (Eq.(5) in main text) are slightly different from those in Ref.[21, 22]. The discrepancy may be induced by their improper use of relative momentum of two colliding fermions (with momenta k_i, k_j), which should be $(k_i - k_j)/2$ rather than $k_i - k_j$. Here, we consider that the correct definition of relative momentum of two colliding fermions is $i(k_j - k_l)/2 \sim \partial_x$, which gives rise to Eq.(5) in our paper. However, the BAEs in Ref.[21, 22] are consistent with ours if the transformation $\xi_p \rightarrow \xi_p/2$, $1/l_p \rightarrow 2/l_p$ is applied.
- [26] V. Gurarie, Phys. Rev. A **73**, 033612 (2006).
- [27] R. Qi and X.-W. Guan, Europhysics Letters **101**, 40002 (2013).
- [28] A. L. Gaunt, T. F. Schmidutz, I. Gotlibovych, R. P. Smith, and Z. Hadzibabic, Phys. Rev. Lett. **110**, 200406 (2013).